ERDC TR-20-26

US Army Corps
of Engineers®
Engineer Research and
Development Center

ERDC
ENGINEER RESEARCH & DEVELOPMENT CENTER

Mobility in Complex Urban Environments (MCUE)

Snow-Covered Obstacles' Effect on Vehicle Mobility

Mark Bodie, Michael W. Parker, Alex Stott, and Bruce Elder

November 2020

Engineer Research and
Development Center

The U.S. Army Engineer Research and Development Center (ERDC) solves the nation's toughest engineering and environmental challenges. ERDC develops innovative solutions in civil and military engineering, geospatial sciences, water resources, and environmental sciences for the Army, the Department of Defense, civilian agencies, and our nation's public good. Find out more at www.erdc.usace.army.mil.

To search for other technical reports published by ERDC, visit the ERDC online library at https://erdclibrary.on.worldcat.org/discovery.

ERDC TR-20-26
November 2020

Snow-Covered Obstacles' Effect on Vehicle Mobility

Mark Bodie

U.S. Army Engineer Research and Development Center (ERDC)
Information Technology Laboratory (ITL)
72 Lyme Road
Hanover, NH 03755-1290

Michael W. Parker, Alex Stott, and Bruce Elder

U.S. Army Engineer Research and Development Center (ERDC)
Cold Regions Research and Engineering Laboratory (CRREL)
72 Lyme Road
Hanover, NH 03755-1290

Final Report

Prepared for Headquarters, U.S. Army Corps of Engineers
Washington, DC 20314-1000

Under Mobility in Complex Environments
PE 622145 / Project BG2 / Task 02, "Cold Regions Effects in Urban Environments"

Abstract

The Mobility in Complex Environments project used unmanned aerial systems (UAS) to identify obstacles and to provide path planning in forward operational locations. The UAS were equipped with remote-sensing devices, such as photogrammetry and lidar, to identify obstacles. The path-planning algorithms incorporated the detected obstacles to then identify the fastest and safest vehicle routes. Future algorithms should incorporate vehicle characteristics as each type of vehicle will perform differently over a given obstacle, resulting in distinctive optimal paths.

This study explored the effect of snow-covered obstacles on dynamic vehicle response. Vehicle tests used an instrumented HMMWV (high mobility multipurpose wheeled vehicle) driven over obstacles with and without snow cover. Tests showed a 45% reduction in normal force variation and a 43% reduction in body acceleration associated with a 14.5 cm snow cover. To predict vehicle body acceleration and normal force response, we developed two quarter-car models: rigid terrain and deformable snow terrain quarter-car models. The simple quarter models provided reasonable agreement with the vehicle test data. We also used the models to analyze the effects of vehicle parameters, such as ground pressure, to understand the effect of snow cover on vehicle response.

Contents

Figures and Tables

Figures

Tables

Preface

This study was conducted for the U.S. Army Corps of Engineers under Mobility in Complex Environments PE 622145 / Project BG2 / Task 02, "Cold Regions Effects in Urban Environments." The technical monitor was Mr. Josh R. Fairley.

The work was performed by the Computational Analysis Branch (CAB) of the Computational Science and Engineering Division (CSED), U.S. Army Engineer Research and Development Center, Information Technology Laboratory (ERDC-ITL). The work was also performed by the Force Projection and Sustainment Branch (FPSB), the Engineering Resources Branch (ERB), and the Terrestrial and Cryospheric Sciences Branch (TCSB) of the Research and Engineering Division (RED), ERDC Cold Regions Research and Engineering Laboratory (CRREL). At the time of publication, Dr. Jeffery L. Hensley was Chief, CAB; Dr. Jerrell R. Ballard Jr. was Chief, CSED; Mr. Jared I. Oren was Chief, ERB; Dr. John W. Weatherly was Chief, TCSB; Mr. J. D. Horne was Acting Chief, FPSB, and Chief, RED. The Deputy Director of ERDC-ITL was Ms. Patti S. Duett, and the Director was Dr. David A. Horner. The Deputy Director of ERDC-CRREL was Mr. David B. Ringelberg, and the Director was Dr. Joseph L. Corriveau.

COL Teresa A. Schlosser was Commander of ERDC, and Dr. David W. Pittman was the Director.

Acronyms and Abbreviations

CAB	Computational Analysis Branch
CRREL	Cold Regions Research and Engineering Laboratory
CSED	Computational Science and Engineering Division
ERB	Engineering Resources Branch
ERDC	U.S. Army Engineer Research and Development Center
FPSB	Force Projection and Sustainment Branch
HMMWV	High Mobility Multipurpose Wheeled Vehicle
ITL	Information Technology Laboratory
MCE	Mobility in Complex Environments
RED	Research and Engineering Division
TCSB	Terrestrial and Cryospheric Sciences Branch
UAS	Unmanned Aerial Systems

1 Introduction

1.1 Background

The Mobility in Complex Environments (MCE) project used unmanned aerial systems (UAS) to identify obstacles and to provide path planning in forward operational locations. The UAS was equipped with lidar and visual imagery for photogrammetry to identify obstacles. The path-planning algorithms incorporated the detected obstacles to then identify the fastest and safest vehicle routes. Ideally, the optimal route would be identified in near real time, enabling obstacles placed by an opposing force to be identified and mitigated. Future algorithms should incorporate vehicle characteristics as each type of vehicle will perform differently over a given obstacle, resulting in distinctive optimal paths.

Terrain differences generate unique challenges in obstacle detection and vehicle mobility. For example, snow cover can obscure obstacles, making detection difficult. The vehicle's dynamic response is different for obstacles that are snow covered compared to obstacles without snow cover. This work focuses on the vehicle's dynamic response to snow-covered obstacles and presents a means to predict the response. This study used the predicted vehicle's dynamic response in conjunction with the obstacle detection and path-planning algorithms to identify the optimal path for a given vehicle.

For the MCE project, researchers at the U.S. Army Information Technology Laboratory (ITL) and the Cold Regions Research and Engineering Laboratory (CRREL) investigated both using UAS sensing technologies to detect snow-covered obstacles and determining the obstacles' impact on vehicle mobility. The project collected photogrammetry and lidar data at two obstacle-laden sites. We used the photogrammetry and lidar data to generate digital elevation models of the sites. A number of photogrammetry experiments, using a UAS, were conducted to determine the optimal camera filter setting (830NIR) for resolving snow-covered obstacles. This project then developed obstacle detection algorithms from the photogrammetry-generated digital elevation models. A number of methods were investigated, including edge detection and texture detection. As part of this project, Vecherin et al. (2020) found that the texture method generated better results than the edge-detection method, allowing the detection of snow-

covered obstacles with fewer false positives. It developed an additional algorithm to determine the probability of false positives. Vecherin et al. (2020) fully describes the obstacle detection algorithms.

Winter conditions, specifically snow cover, represent unique challenges to vehicle mobility. Increased motion resistance reduces net traction available for vehicle motion. Greater snow depths reduce or eliminate available vehicle ground clearance. With ground clearance eliminated, the snow supports the vehicle, reducing the normal force on the wheels. In addition, the vehicle motion resistance further increases from snowplowing. In snow, gross traction is lower than in most other terrains as both the low friction coefficient and internal shear strength of snow reduces the available traction (Blaisdell et al. 1990; Richmond et al. 1990, 1995).

In addition to the above challenges, snow can also obscure obstacles, making identification of an optimal path difficult. Unidentified obstacles can immobilize vehicles or cause operator and equipment vibration to exceed limits if driven over at excessive speed. The vehicle's lateral stability is also adversely affected by large normal force variations over rough surfaces. Each effect will reduce the safe operating speed, effecting the optimal path of the vehicle.

1.2 Objective

This research explored the effect of snow-covered obstacles on dynamic vehicle response. The objective was to understand and predict the vibratory response of the vehicle given the obstacle size and snow-cover conditions. The predictive methods described in this study will be used in future optimal path planning tools.

1.3 Approach

The investigation began by conducting vehicle tests using an instrumented HMMWV (high mobility multipurpose wheeled vehicle). The tests involved driving over obstacles of different sizes, with and without snow cover. Data acquisition systems on board the vehicle recorded a number of vehicle sensor signals, including vehicle speed, body acceleration, and wheel forces. We took various snow characteristic measurements (e.g., snow depth and density). Snow depths were measured in both the virgin snow and the ruts generated by the vehicle. Section 2 provides a full description of the vehicle testing.

We developed two simple quarter-car models to predict the vehicle's vertical body acceleration and wheel normal force. The first quarter-car model developed was the well-known rigid terrain quarter-car model (Karnopp 1990; Pavlov 2017; Mehmood 2014). The second quarter-car model developed incorporated a deformable snow surface over rigid terrain. Section 3 describes each model. We compared the results from each model to one another and to the vehicle test data (section 4). Model studies (section 5), showed the effects snow cover had on vehicle vibratory response for a low-ground-pressure vehicle and for ground profiles with varying frequencies. Finally, the Conclusions and Recommendations section provides the main results of the work and recommendations for future work.

2 Vehicle Testing

This study conducted a number of vehicle dynamics tests at CRREL in the northwestern sector on the campus (Figure 1). An instrumented HMMWV was tested over three different-sized obstacles with and without snow cover. The obstacles were commercial portable speed bumps that closely resemble a circular chord. All obstacles were secured with bolted anchors in the concrete pad. Table 1 provides the dimensions for each bump. Figure 2 shows each bump as installed and tested.

Figure 1. Overhead view of the CRREL campus (*left*), highlighting the concrete pad used as a test area (*right*). The test site was cleared of most equipment and structures before testing.

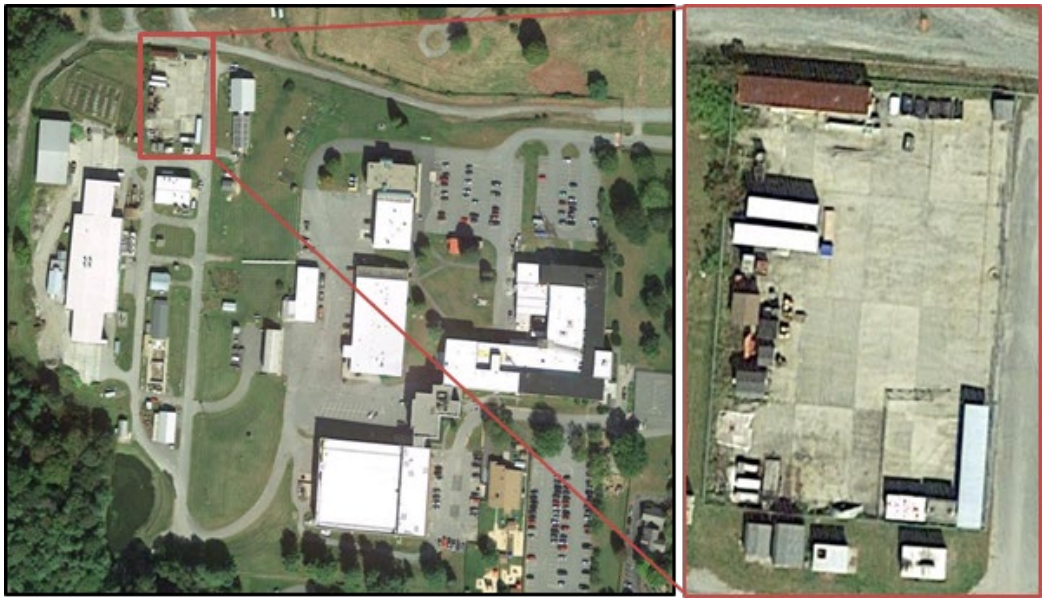

Table 1. Obstacle dimensions in centimeters.

Obstacle	Height	Chord Length	Length
Speed Bump 1	7.62	30.5	365.8
Speed Bump 2	4.76	30.5	365.8
Speed Bump 3	4.92	91.4	365.8

Figure 2. Speed bumps installed on the concrete pad referenced in Fig. 1.

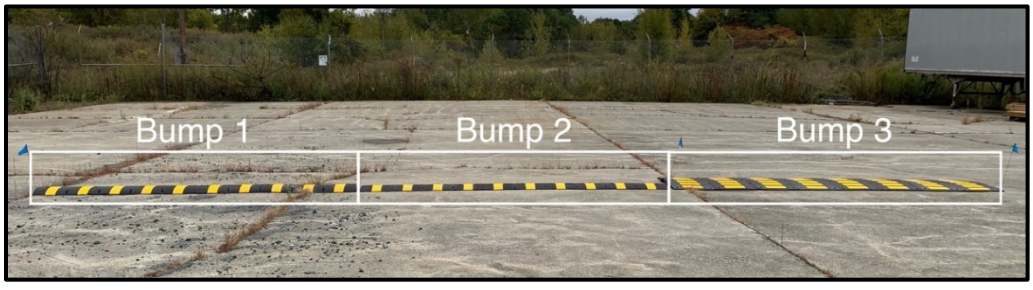

The instrumentation installed on the HMMWV included the following sensors (Figure 3):

1. AiM EVO5 data acquisition system with GPS
2. Pegasus Fifth Wheel
3. HBM MGCplus data acquisition system
4. Wheel Force Transducers

The AiM EVO5 is a data acquisition system that contains a built-in inertial measurement unit capable of measuring six degrees of freedom: linear accelerations in x, y and z, as well as roll, pitch, and yaw rates. It is also capable of recording a 10 Hz* GPS signal, providing location and vehicle speed using a GPS puck attached to the roof of the vehicle. The EVO5 contains eight possible analog ports with a maximum sampling frequency of 1 kHz.

Figure 3. The data acquisition systems on board the HMMWV (*left*) and the fifth wheel attached to the rear of the vehicle (*right*).

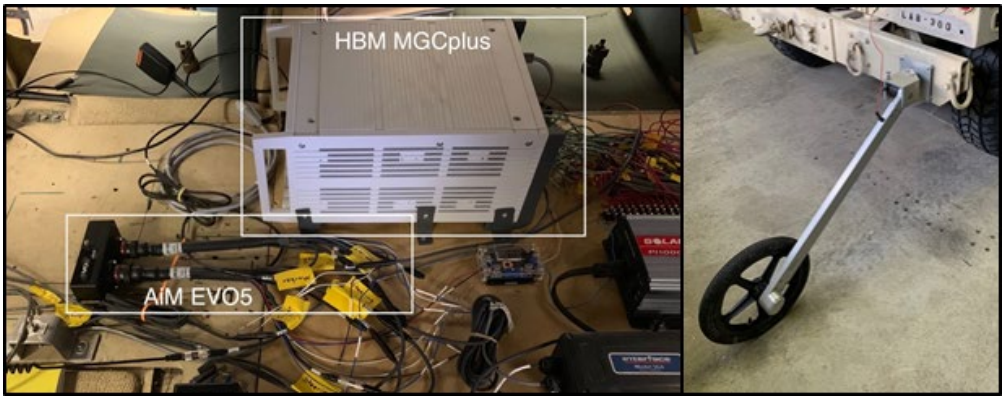

A fifth wheel (Figure 3) was attached to the rear of the HMMWV and connected to the AiM system to obtain direct vehicle speed measurements, which are more accurate than the calculated GPS speed. For these tests, the sampling rate was set to the maximum of 100 Hz for the linear accelerations and vehicle speed, 50 Hz for the rotational rates, and 10 Hz for the GPS. The data was interpolated during postprocessing to obtain a 100 Hz signal for all instrumentation signals.

The HMMWV used has an HMB MGCplus data acquisition system installed, which is used to record the force and rotation measurements for

* For a full list of the spelled-out forms of the units of measure used in this document, please refer to *U.S. Government Publishing Office Style Manual*, 31st ed. (Washington, DC: U.S Government Publishing Office, 2016), 248–252, https://www.govinfo.gov/content/pkg/GPO-STYLEMANUAL-2016/pdf/GPO-STYLEMANUAL-2016.pdf.

each of the four vehicle wheels. Each wheel also has a force transducer system installed, composed of six load cells, three oriented laterally and three longitudinally and vertically, to measure the forces and moments on the wheel (Figure 4). An encoder held in place by an aluminum frame that wraps over the tire records the rotation of the wheel. The information for the 24 load cells and 4 encoders transmits wirelessly from each wheel to 28 receivers inside the vehicle that connect to the HBM system.

Figure 4. A wheel force transducer unit installed on one of the wheels of the HMMWV with transmitters and the encoder reference bar (*left*), and one of four receiver units installed inside the HMMWV (*right*).

For relatively consistent test conditions across all bumps, we removed from the test site any snow present before a major snow event. This helped to promote a constant snow depth before, on, and after each bump. To maximize iterations, the vehicle was driven closer to the left side of the bump for the first run. Then, the vehicle was driven closer to the right side of the bump for the second run so that the driver's-side wheels split the old tracks. This resulted in two runs per bump for each major snow event.

At the start of each run, we activated the recording systems; and the HMMWV was accelerated to a relatively constant speed before hitting a bump. For Bumps 1 and 2, the desired speed was 8 km/h. To ensure a measurable signal, the tests for Bump 3 required reaching a speed of 16 km/h before reaching the bump. After hitting a bump, the vehicle was slowed to a stop, the recording systems were stopped, and the data were saved. The vehicle was then moved into position for the next run.

During the vehicle tests, we dug multiple snow pits in the testing area to measure snow depth, density, moisture, and temperature. These values are needed to create relationships between the snow cover over the bumps and the damping effect it has on the vehicle.

Once all vehicle testing was complete, we took snow- and rut-depth measurements on and parallel to the bumps. We then removed snow from the bumps and surrounding area so that plows could clear the test site without damaging the equipment. This final step allowed for clear test conditions for the next snowfall.

We conducted the baseline tests (no snow) on 4 April 2019 and snow-covered testing on 13 February 2019. Additional testing days did take place earlier in the season, but the data was unusable due to signal interference issues with other equipment. This caused incomplete collection of wheel-force data, rendering it unusable. It was not until later on in testing that we identified the source of the issue and corrected it so that successful data could be collected for the final significant snowfall of the season.

The snow-covered testing data showed substantial reductions in normal force variation and body acceleration as can be seen in Figures 5 and 6. A snow depth of 16 cm reduced the normal force variation over Bump 1 by 45% and the body acceleration by 43%.

Figure 5. Normal force comparison with and without snow: Bump 1.

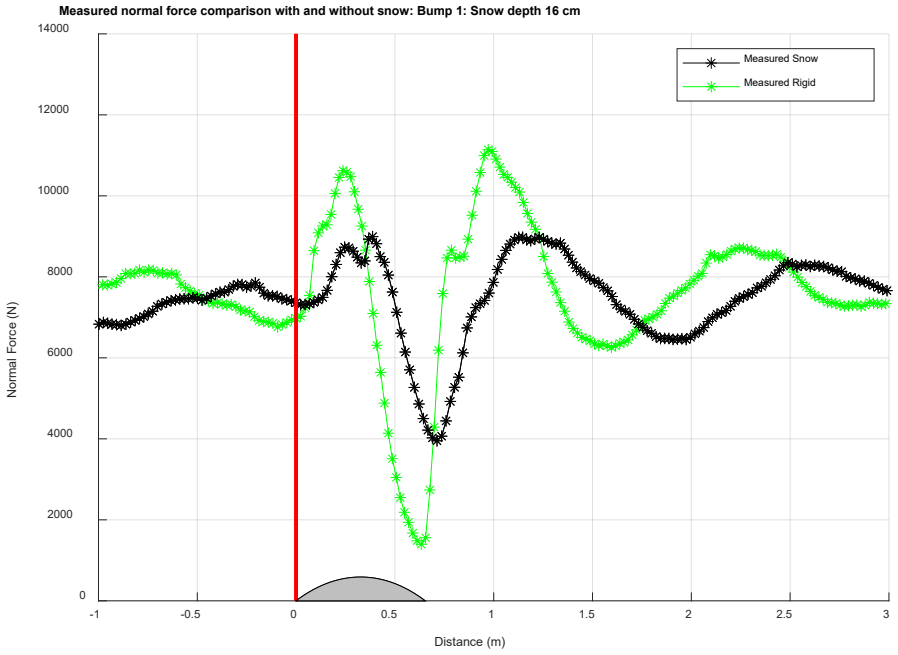

Figure 6. Sprung acceleration comparison with and without snow: Bump 1.

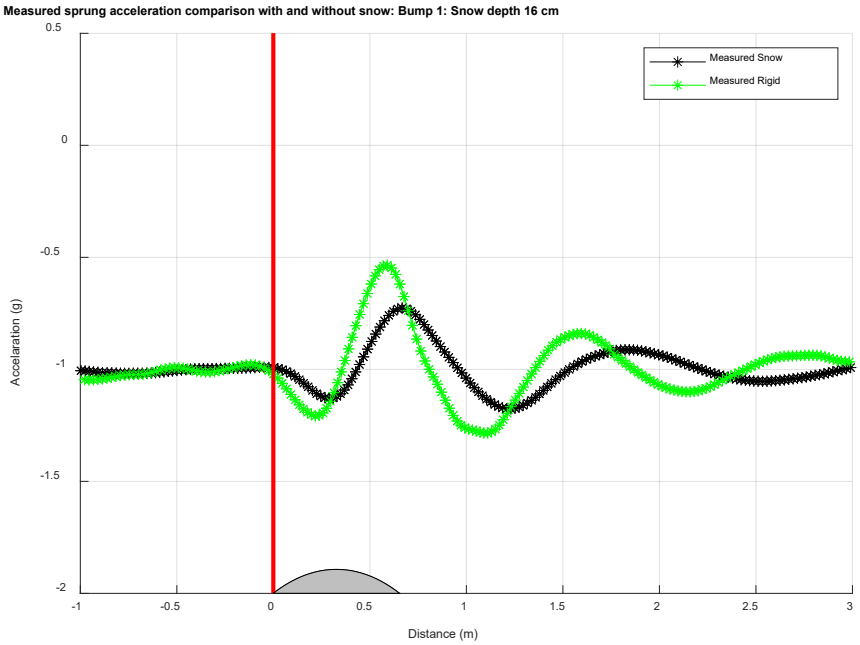

3 Quarter-Car-Model Description

We developed rigid-surface and deformable-snow-surface quarter-car models to predict the vehicle's vertical body acceleration and wheel normal force. The well-known rigid quarter-car model is composed of two degrees of freedom: the sprung (body) mass and the unsprung (wheel) mass vertical positions. The sprung and unsprung masses are connected through the suspension spring and damper, and the unsprung mass is connected to the road surface through the tire spring (Figure 7). A quarter-car model is a gross simplification of an actual vehicle, capturing only vertical displacements of the vehicle. The model ignores angular rates and yaw-plane dynamics as well as secondary sprung masses on the vehicle, such as the engine, which can significantly affect the vibration response of the vehicle. Although a simplification, a quarter-car model captures the major vibration response of the vehicle with a minimal number of parameters. The model has been used extensively to understand vehicle-ride characteristics and controllable suspension systems (Karnopp 1990; Pavlov 2017; Mehmood 2014).

Figure 7. Quarter-car model.

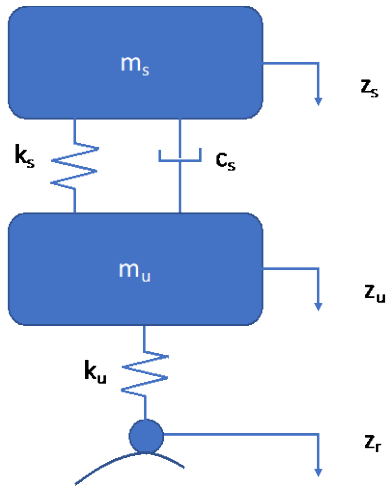

In this work, we developed a state-space representation of the quarter model, or

$$\begin{Bmatrix} \dot{z}_s \\ \dot{z}_u \\ \ddot{z}_s \\ \ddot{z}_u \end{Bmatrix} = \begin{bmatrix} 0 & 0 & 1 & 0 \\ 0 & 0 & 0 & 1 \\ -k_s/m_s & k_s/m_s & -c_s/m_s & c_s/m_s \\ k_s/m_u & -(k_u + k_s)/m_u & c_s/m_u & -c_s/m_u \end{bmatrix} \begin{Bmatrix} z_s \\ z_u \\ \dot{z}_s \\ \dot{z}_u \end{Bmatrix} + \begin{bmatrix} 0 \\ 0 \\ g \\ g + k_u z_r/m_u \end{bmatrix}, \quad (1)$$

where

k_s = the suspension spring,
c_s = the suspension damper,
m_s = the sprung mass,
g = gravity,
k_u = the unsprung stiffness,
z_s = the sprung mass position,
z_u = the unsprung mass position, and
z_r = the road profile.

The normal force is calculated by multiplying the unsprung stiffness by the difference between the unsprung mass position and the road profile, or

$$F_n = k_u(z_u - z_r), \tag{2}$$

where F_n is the vehicle's normal force on the surface. The initial conditions for the quarter-car model are determined by equating the sprung and unsprung velocities and accelerations to zero and solving for the sprung and unsprung displacements, or

$$\begin{Bmatrix} z_s \\ z_u \end{Bmatrix} = \begin{bmatrix} -k_s/m_s & k_s/m_s \\ k_s/m_u & -(k_u + k_s)/m_u \end{bmatrix}^{-1} \begin{bmatrix} g \\ g + k_u z_r/m_u \end{bmatrix}. \tag{3}$$

For the deformable snow-surface quarter-car model, the vehicle's ground pressure equals the snow strength. The snow strength is a function of the vehicle sinkage depth. To determine the snow strength, we used a modified Wong sinkage equation, or

$$z = z_w \left[1 - e^{\left(-\frac{P_c}{P_w}\right)}\right], \tag{4}$$

$$P_w = C_r \, \rho_o, \tag{5}$$

$$z_w = h \left[1 - \frac{\rho_o}{\rho_{f\left[1+b_s/b\right]}}\right], \tag{6}$$

where

P_c = the vehicle's ground pressure;
P_w = the snow strength, which is a function of snow density;
h = the snow depth;
b = the tire or track width;
z_w = the maximum asymptotic sinkage;
z = the sinkage depth; and
ρ_0 = the initial snow density.

C_r, ρ_f, and b_s are regression constants:

C_r = 48.36 kPa/(g/cc),
ρ_f = 0.416604 g/cc,
b_s = 0.614817 m.

Shoop et al. (2019) detail the modified sinkage equation.

We note that the vehicle ground pressure is equal to the normal force divided by the tire contact area, A_c. For the quarter-car model, we assume that the tire contact area remains constant and note that the unsprung position is a state and is available at each integration step.

$$P_c = {N_F}/{A_c} = {k_u}/{A_c}\ (z_u - z_r). \tag{7}$$

We also rearrange equation (4) and then equate the vehicle ground pressure and solve for sinkage depth (road profile), or

$$P_c = P_w \left[-ln\left(1 - \frac{z_r}{z_w}\right)\right], \tag{8}$$

$$P_w \left[-ln\left(1 - \frac{z_r}{z_w}\right)\right] = {k_u}/{A_c}\ (z_u - z_r), \tag{9}$$

$$e^{\left[\frac{{k_t}/{A_c}}{P_w}(z_r - z_w)\right]} + \frac{z_r}{z_w} - 1 = 0. \tag{10}$$

Equation (8) is numerically solved for the root z_r. Because the quarter-car model is coded in MATLAB, we vectorize z_r for all feasible values from zero

to z_w in increments of 0.25 mm. We next generate the error vector and use the "interp1()" function with the error vector as the x argument and the z_r vector as the y argument. We then set the desired error to zero and determine the root, z_r.

4 Experimental Data Prediction Comparison

In this section, we compare the quarter model results to experimental measured data from CRREL's instrumented HMMWV. We compare the deformable snow-surface quarter-car model's predicted normal force and body acceleration to experimental test data collected on 13 February 2019. We compare the rigid-surface quarter-car model's predictions to experimental data collected on 4 April 2019. Additionally, we compared the deformable snow quarter-car model to the rigid quarter-car model by using minimal snow cover and low snow density. In such a configuration, the deformable snow-surface model should have a similar response to the rigid-surface quarter-car model. We also identify assumptions and modifications required for the quarter-car model to have good agreement with the experimental data.

The largest assumption associated with a quarter-car model is that the vehicle dynamics can be reduced to two degrees of freedom, vertical motion of the sprung (body) and unsprung (wheel) masses. It ignores all other vehicle degrees of freedoms. The model has no mechanism to predict vehicle pitch or roll motion or lateral and longitudinal motions. Although, the quarter-car model has major limitation in predicting vehicle motion, the model's simplicity reduces the model inputs to a minimum and predicts the important body acceleration and tire normal force. With the study's objective to determine the effect of snow-covered obstacles on the vehicle's dynamic response, the deformable snow-surface algorithm is the unique and most important feature of the model. The deformable snow-surface algorithm can in the future be applied to vehicle models with greater degrees of freedom. We will show later in this section that the quarter-car-model predictions reasonably compare to the measured data.

The quarter-car model also assumes that the tire spring follows the road surface as a point (Figure 7). In the actual vehicle, the wheel diameter modifies the road profile by increasing the obstacle width and reducing its height. Consider a rigid wheel striking an obstacle (Figure 8).

Figure 8 shows that the wheel does not follow the exact profile of the obstacle. The wheel strikes the obstacle at a point above the obstacles interface with the surface. The change in the obstacle height and chord can be determined using Figure 9.

Figure 8. Rigid wheel obstacle profile.

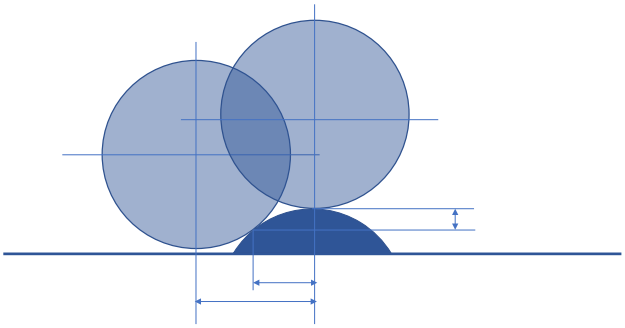

Figure 9. Modification of obstacle height and chord.

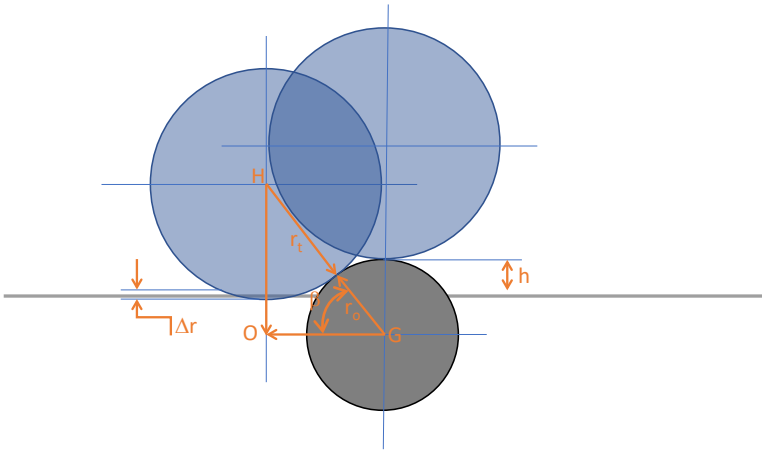

The modified chord length is calculated from the length of line, *OG*, and the obstacle height is the difference between the bump height and the tangent point between the tire and the obstacle. Line length, *HO*, is given by the sum of the tire and obstacle radius minus the obstacle height, h, and the tire deflection, Δr, or

$$HO = r_t + r_o - \Delta r - h. \tag{11}$$

The half chord length is given by Pythagorean's theorem, or

$$OG = \sqrt{(r_t + r_o)^2 - (r_t + r_o - \Delta r - h)^2}. \tag{12}$$

Using the law of sines, the angle between line segments *OG* and *HG* is determined, or

$$\beta = \sin^{-1}\left(\frac{r_t + r_o - \Delta r - h}{r_t + r_o}\right). \tag{13}$$

The modified obstacle height is given as

$$h_m = r_o - (r_o \sin(\beta)). \tag{14}$$

In the quarter-car comparison, the obstacle profiles used were modified to reflect the difference in point- and wheel-following profiles.

The quarter-car models used in this work were linear; the sprung stiffness, unsprung stiffness, and damping coefficient were assumed to be linear. This simplification was made to limit the model's required parameter information. The additional information may or may not be available; and the simplified vehicle model, which uses only two degrees of freedom, does not warrant additional suspension-parameter fidelity.

The left front body spring and tire rates were measured using vehicle scales. The spring stiffnesses were 79,000 N/m (body) and 339,000 N/m (tire). The quarter-car model used the measured spring rates as the sprung and unsprung stiffness. The estimated unsprung mass was 65 kg. The tire width was 0.33 m, and a damping coefficient of 4325 N/(m/s) was selected. The above parameters result in a sprung natural frequency of 1.74 Hz, unsprung natural frequency of 11.5 Hz, and a percent critical damping of 42%.

For a no-snow condition, the deformable snow quarter-car model and rigid quarter-car results should converge. To simulate a no-snow condition, we modeled low-snow-strength conditions, reducing the snow density to 0.02 g/cc at a depth of 5 cm. Figures 10 and 11 show the converged deformable and rigid quarter-car-model results.

Figure 10. Rigid and deformable snow quarter model comparison for shallow low-density snow: normal force.

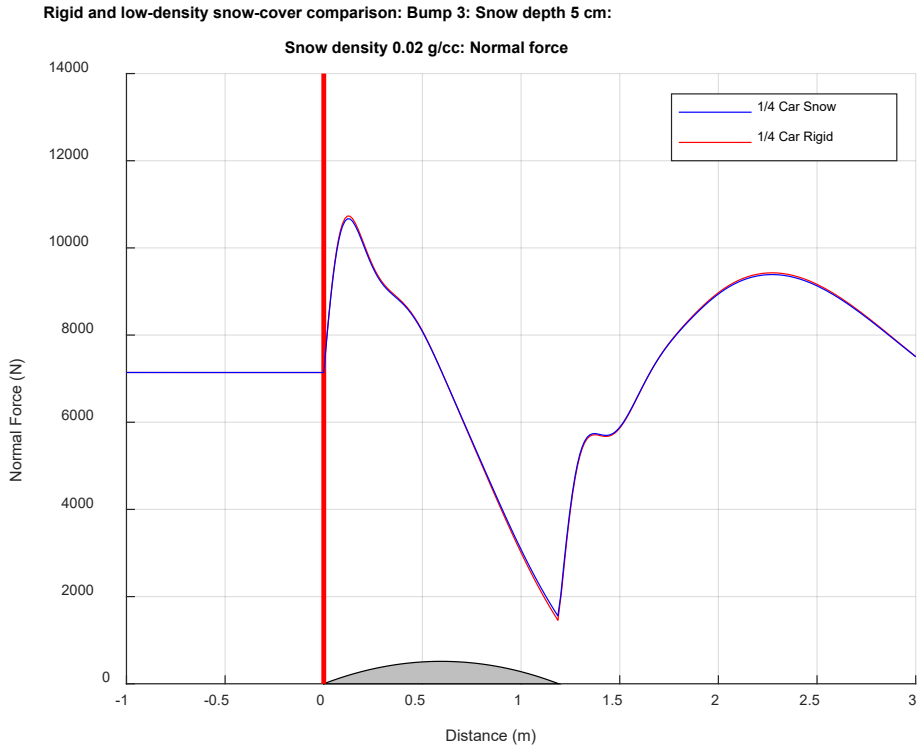

Figure 11. Rigid and deformable snow quarter model comparison for shallow low-density snow: rut depth.

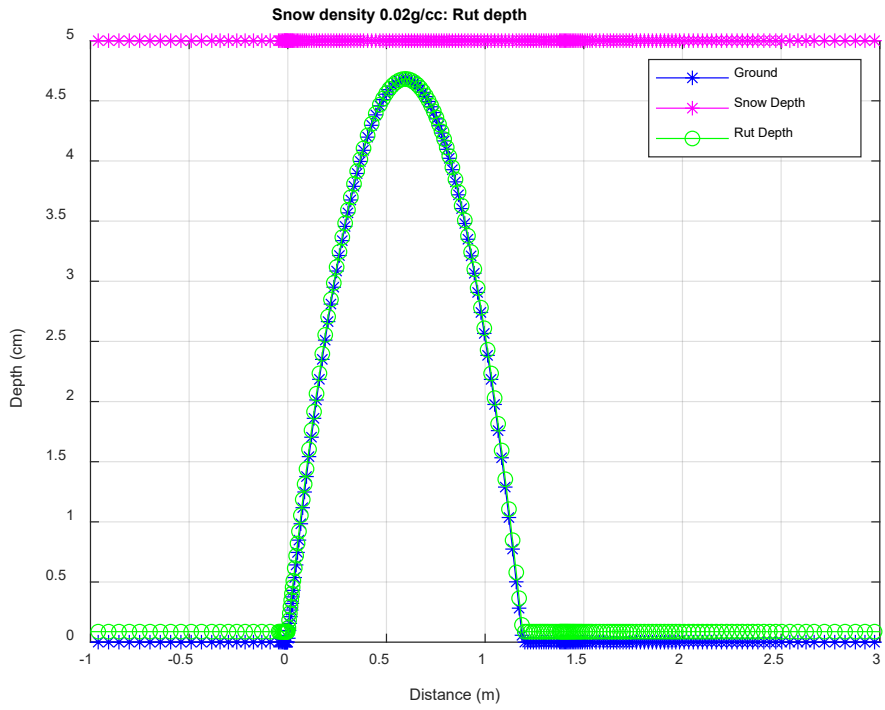

Figures 12 through 14 compare measured and predicted normal force for snow and no-snow conditions for Bumps 1 through 3. Bump 3, the shallowest obstacle, provided the best comparison between the measured and model-predicted normal force. For the rigid case, the model predicted within 9% of the measured normal force variation. For the snow case, the model predicted within 23% of the measured normal force variation. The difference in the predicted accuracy between obstacles can be attributed to the point-following assumption associated with the quarter-car model. The profiles associated with Bump 1 and 2 change more dramatically than for Bump 3, which is much wider (91.4 cm) than Bumps 1 and 2 (30.5 cm)

The normal force predictions for Bump 1 and 2 also underestimated the effect of the snow on normal force variation. The lack of accuracy in the predicted normal force may be attributed to the vertical-only assumption of the quarter-car model. In general, the quarter-car model followed the trends of the measured values, and snow-covered obstacles always resulted in smaller normal force variation. The best predictions between the quarter-car model and measured values were associated with the shallowest obstacle.

Figure 12. Normal force comparison for Bump 1.

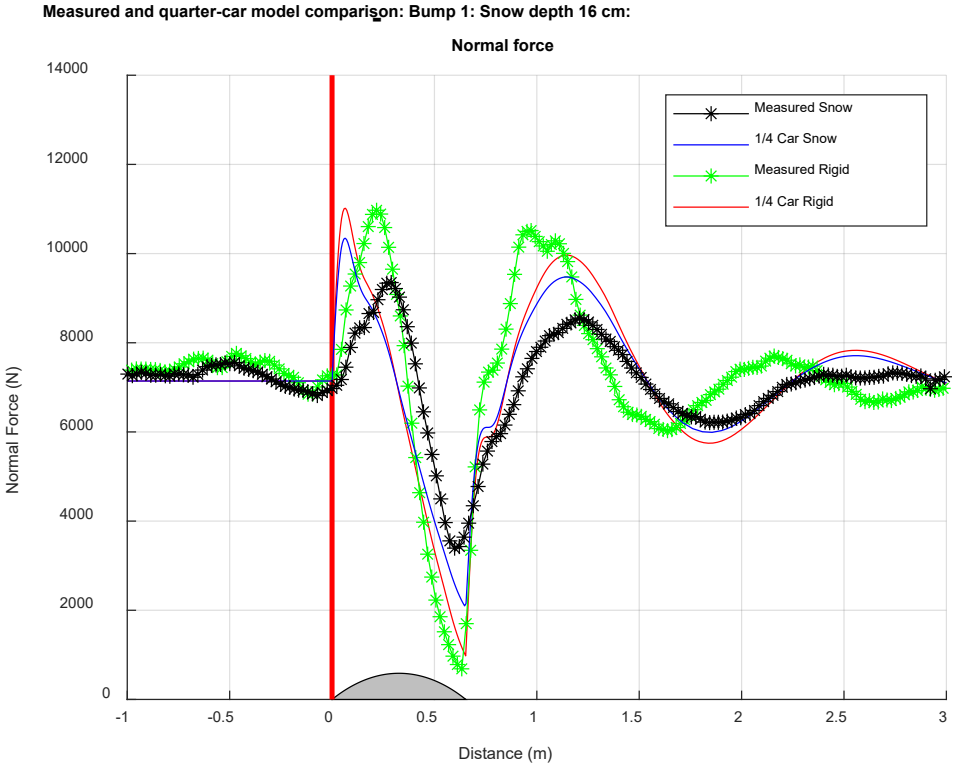

Figure 13. Normal force comparison for Bump 2.

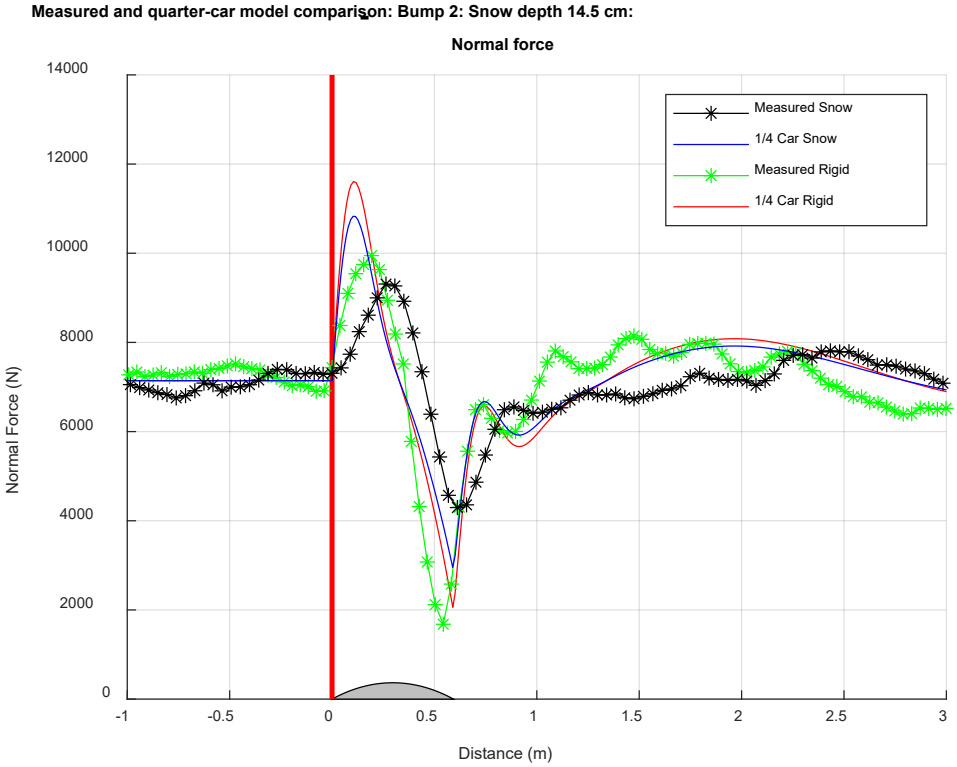

Figure 14. Normal force comparison for Bump 3.

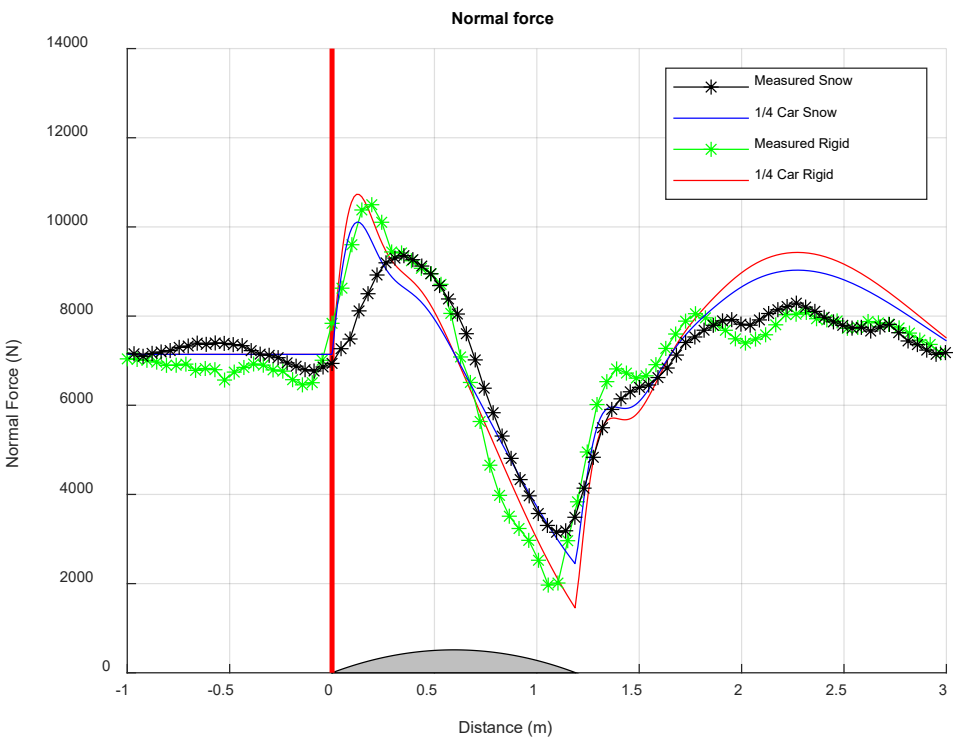

Figures 15 through 17 compare measured and predicted rut depths. The predicted rut depths compare favorably with the measured rut depth with the predicted values falling within 0.7 cm of the measured values for all three obstacles.

The snow-covered conditions reduced the vehicle's dynamic response by modifying the profile that the vehicle traversed. The abruptness of the ground profile is reduced as the compressed snow fills areas around the obstacle. Section 5 demonstrates this phenomenon more dramatically with a simulated low-ground-pressure vehicle. With low-ground-pressure vehicles, the compressed snow rut profile is dramatically altered when compared to the ground profile (Figure 20).

Figure 15. Rut-depth comparison for Bump 1.

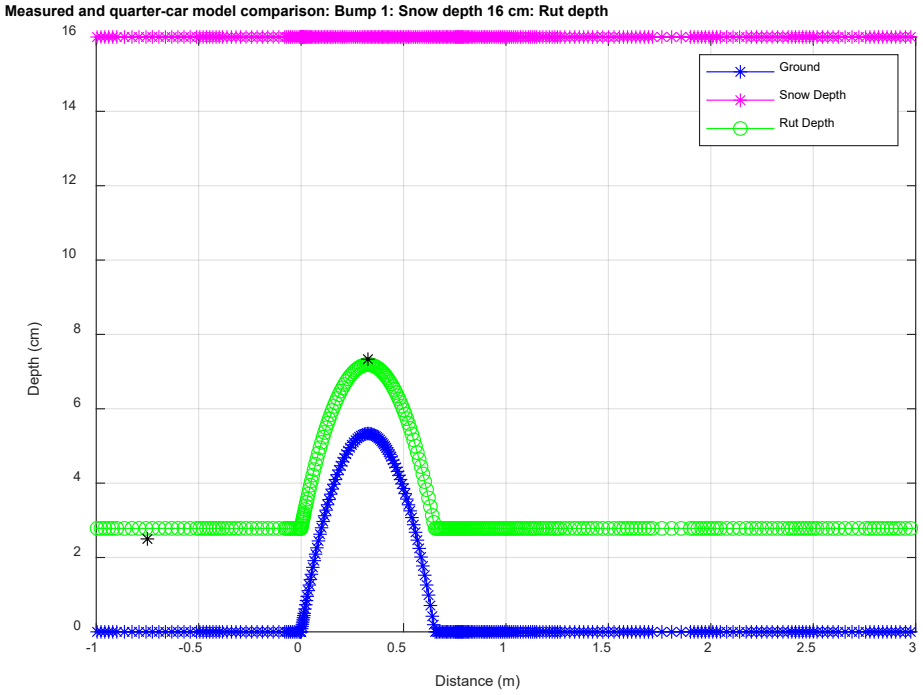

Figure 16. Rut-depth comparison for Bump 2.

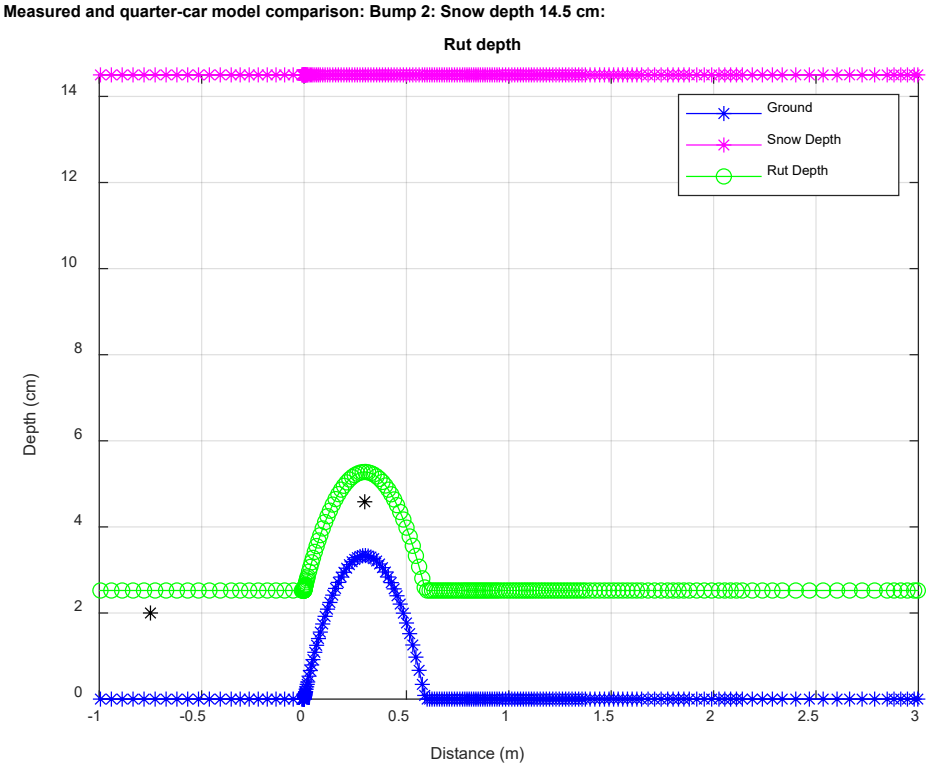

Figure 17. Rut-depth comparison for Bump 3.

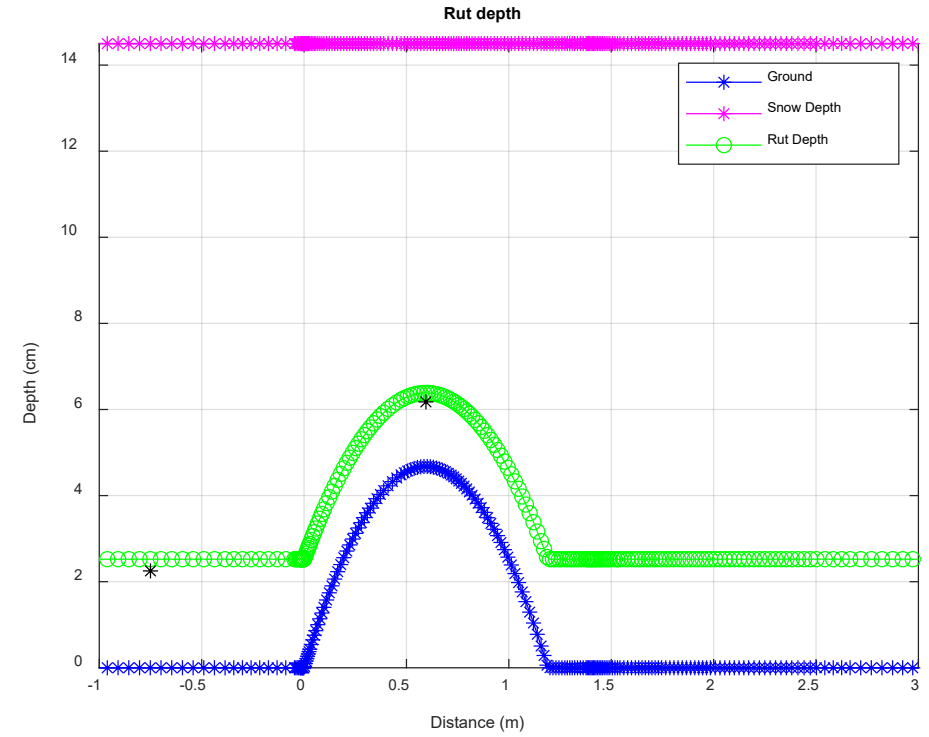

The measured and predicted body acceleration did not compare favorably with one another as seen in Figure 18. The measured body acceleration is lower than the predicted body acceleration. The simplicity of the quarter-car model may be the cause of the differences. Future work should investigate models with increased degrees of freedom, such as a half car model, to improve body-acceleration predictions. The body-acceleration difference may also be associated with secondary isolation systems, such as body mounts, on the HMMWV. We recommend using acceleration measurements at the frame and inside the cabin to identify the effect of the secondary isolation system on body acceleration. In addition, measurements with wheel accelerometers could be used to further validate the model.

Figure 18. Body-acceleration comparison for Bump 3.

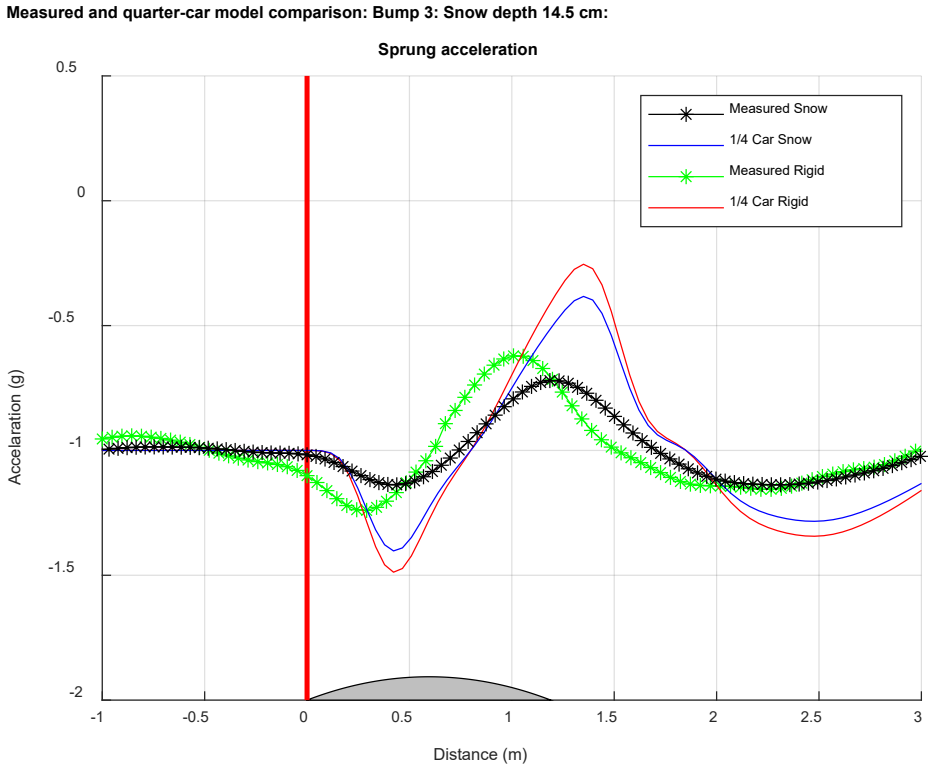

5 Model Analysis

The simple quarter-car model can be used to predict normal force and body acceleration for different terrain conditions and vehicle parameters. This section presents simulation of a low-ground-pressure vehicle. The low-ground-pressure vehicle, 13.8 kPa, has the same vibration characteristics as the HMMWV parameters provided above: sprung natural frequency of 1.74Hz, unsprung natural frequency of 11.5Hz, and 42% of critical damping. We selected for the simulation a snow depth of 30.5 cm with a density of 0.25 g/cc.

Figure 19 compares the normal force variation associated with a low-ground-pressure vehicle for snow and no-snow conditions. The 30.5 cm snow cover reduced the normal force variation by 76%. Figure 20 shows the predicted rut depth. The figure shows the radically modified profile that the vehicle travels over in snow conditions as compared to no-snow conditions. The rut profile difference is the reason for the dramatic reduction in normal force variation in the snow condition. The simulation demonstrates that the snow cover can improve mobility for low-ground-pressure vehicles. It would be beneficial to conduct low-ground-pressure-vehicle testing to further validate the deformable snow quarter model.

Figure 19. Snow and no-snow normal force comparison for a low-ground-pressure vehicle.

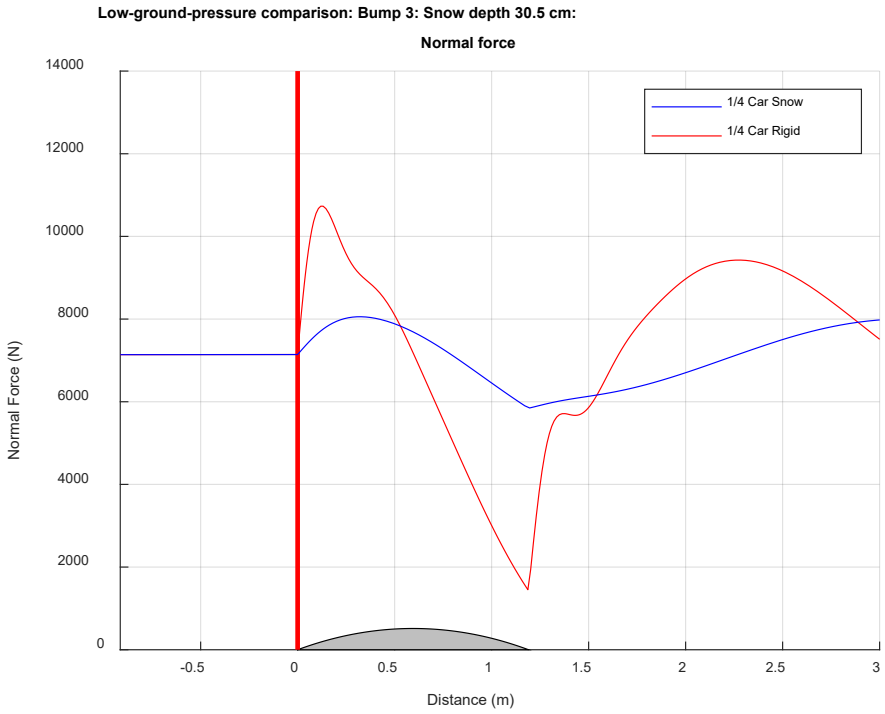

Figure 20. Rut profile for a low-ground-pressure vehicle.

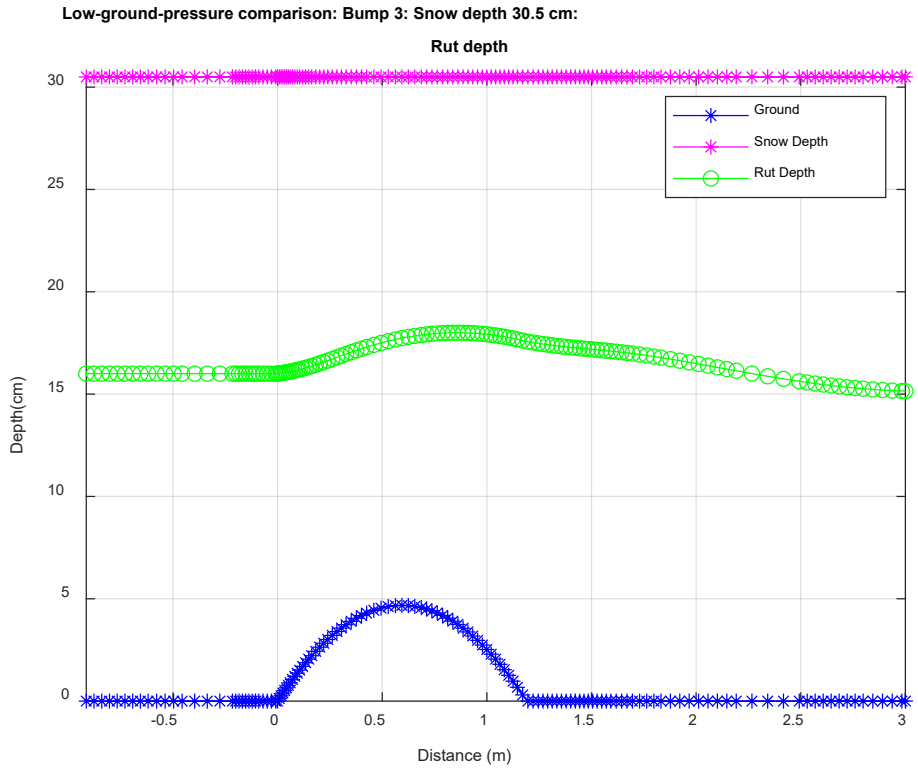

We used a chirp road profile, a frequency-increasing ground profile with time, with the deformable quarter-car model to investigate the effect of snow cover on a vehicle's frequency response. The snow characteristics for the simulation were a 30.5 cm snow depth and a density of 0.25 g/cc. The simulation used the following HMMWV vehicle parameter: sprung natural frequency of 1.74 Hz, unsprung natural frequency of 11.5 Hz, and 42% of critical damping. The chirp ground profile used in the simulation varied from zero to 15 Hz over 60 seconds with an amplitude of 2.54 cm.

Figures 21 and 22 show the body accelerations for the snow and no-snow conditions. Figure 21 compares the snow and no-snow time-domain body accelerations. Figure 22 compares the snow and no-snow body-acceleration power spectral density. The body-acceleration power spectral density was generated using the MATLAB "pwelch()" function with a 50% overlap window for 1.25 Hz to 14 Hz at a 0.05 Hz increment (Oppenheim 1989; Welch 1967). Each figure shows the attenuation of the body acceleration, approximately 2 dB at the lower frequencies, for the snow condition. The attenuation increased at higher frequencies to approximately 4 dB at 14 Hz. The figures also show that the unsprung natural frequency changed

between the snow and no-snow conditions. For the snow condition, the unsprung natural frequency was lowered by 1.5Hz.

Figure 21. Chirp road profile body-acceleration comparison for snow and no snow.

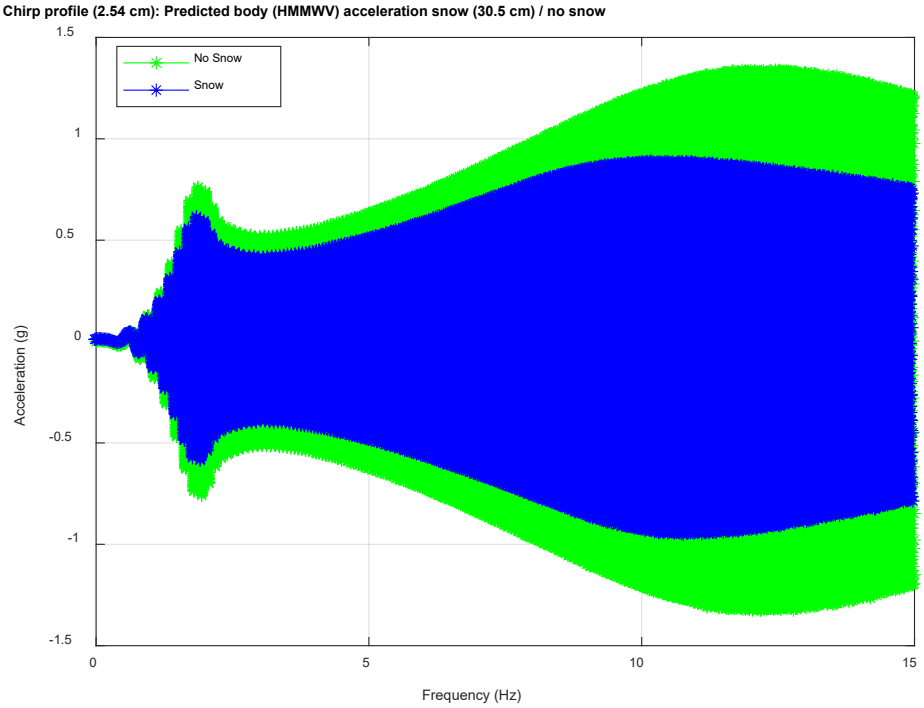

Figure 22. Chirp road profile body-acceleration power spectrum comparison for snow and no snow.

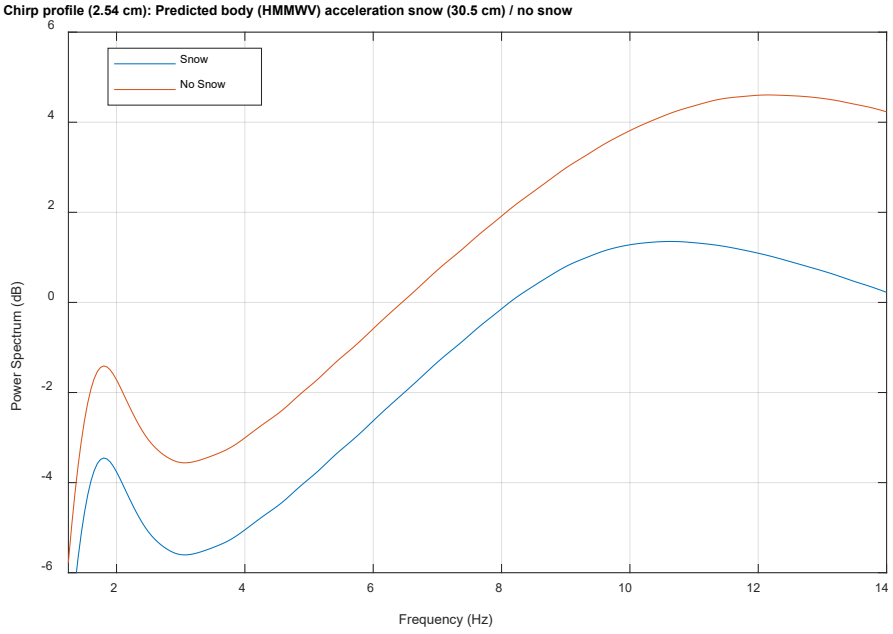

The rut profile variation is reduced as frequency is increased (Figure 23). When the chirp profile reaches the unsprung natural frequency, the variation in normal force is increased. During suspension compression at this frequency, the normal force is at a minimum, resulting in a lower snow sinkage. This effectively reduces the ground profile variation that the vehicle traverses. As with the low-ground-pressure-vehicle testing, it would be beneficial to test with obstacles at varying frequencies to further validate the deformable snow quarter model.

Figure 23. Chirp ground and rut profile comparison with and without snow.

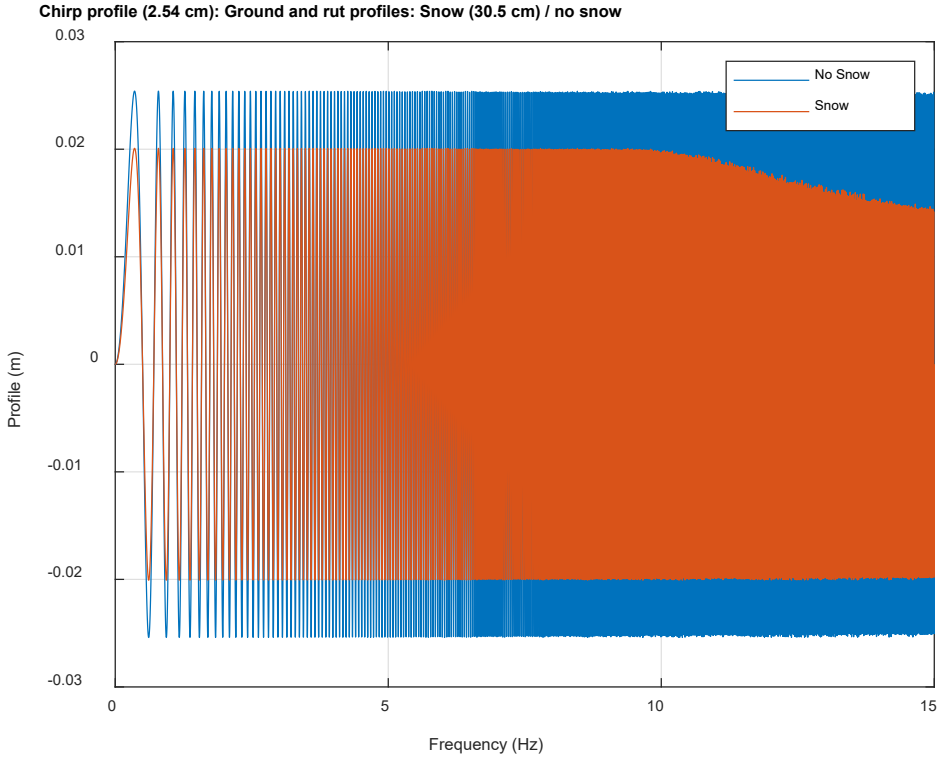

6 Conclusions and Recommendations

Optimal vehicle paths depend not only on the identification of obstacles but also on the interaction between the obstacle and the vehicle. For example, a low-ground-pressure vehicle may be able to transverse low-strength soils where a higher ground pressure vehicle may become immobile due to increase sinkage and motion resistance. A vehicle vibratory response can also have an effect on a vehicle's optimal path. The safe operating speed of a vehicle is limited by the vehicle body acceleration and variation in tire or track normal force. Operator, equipment, and vehicle durability limit the maximum acceptable vehicle body acceleration. Normal force variations directly affect the vehicle's lateral stability. Both body acceleration and normal force variation make optimal vehicle paths dependent on the vehicle's vibration response.

Computer models can simulate large numbers of experiments, which would be prohibitively expensive or impossible to physically test. For example, computer simulations can test various snow conditions that may not occur at the testing location in the allocated testing time. They can simulate vehicles that are otherwise not instrumented or available for testing. The freedom simulations provide allows identification of important parameters and insights that maybe missed in the limited cases available with physical testing.

However, to have confidence in the computer model, the model must be compared to results from physical testing. The more available the testing data over varying conditions, the greater the confidence in the computer model. Additionally, assumptions associated with the computer model need to be highlighted to quantify discrepancies between the computer model and testing data. This will identify conditions where the model has large errors and identify areas to improve the model.

The research presented in this technical report investigated the effect of a vehicle's vibratory response to snow-covered obstacles through vehicle testing and computer simulations. The physical testing of an instrumented HMMWV showed that snow cover has a large effect on the vehicle's vibratory response. The HMMWV traveling at 8 km/h over a 7.62 cm obstacle with a snow depth of 14.5 cm reduced normal force variation by 45% and body accelerations by 43%. We then compared the vehicle test data to rigid and deformable-surface quarter-car models. We used the quarter-car

models to predict normal force variation and vehicle body acceleration over bare and snow-covered obstacles. The models provided reasonable agreement with vehicle test data, following the trends of the measured vehicle data with snow-covered obstacles always resulting in smaller normal force variation. The rigid-surface quarter-car model was able to predict normal force variation within 9% of the measured value. The deformable model predicted normal force variations within 23%. The deformable quarter model provided good predictions of rut depth when compared to measured values, within 0.7 cm for all tests.

The simple quarter-car models require only a few vehicle parameters to estimate a vehicle's vibratory response. The deformable-surface model requires additional parameters for snow depth and density. The quarter-car model's simplicity is a major advantage in implementing the model in existing obstacle detection or path-planning algorithms at the expense of accuracy which is achieved by models with higher degrees of freedom.

The quarter-car model has a number of simplifying assumptions, which limit accuracy. The model reduces a vehicle to two degrees of freedom, body and wheel positions, and also assumes that the tire follows the surface profile as a point. The reduction in the vehicle's body to a single degree of freedom reduced the correlation between the measured and predicted body acceleration. We recommend investigating a half car model, which includes the body-pitch degree of freedom to better predict body acceleration. Differences in predicted and measured body acceleration can also be attributed to secondary isolation systems, such as body mounts. We recommend additional testing with accelerometers at the frame and inside the cabin to identify the effect of secondary isolation systems on body acceleration. In addition, measurements with wheel accelerometers could be used to further validate the model.

Traditional quarter-car models assume that the tire follows the surface as a point. In this study, the point-following profile was modified to a wheel-following profile, which reduces the obstacle's abruptness, increasing obstacle width and reducing obstacle height. Implementing the wheel-following profile reduced the predicted normal force variation and body acceleration compared to the point-following profile, comparing better to the measured data.

Simulation studies were conducted for a low-ground-pressure vehicle, 13.8 kPa, over a bare and a snow-covered obstacle, 4.9 cm height, with a snow depth and density of 30.5 cm and 0.25 g/cc. The simulation with the snow-covered obstacle showed a reduction in normal force variation of 76% over the bare obstacle condition. The large reduction in normal force variation associated with the snow-covered obstacle is from the rut profile being much less abrupt than the ground surface profile. This shows that the mobility of a low-ground-pressure vehicle can be improved with snow cover.

We conducted a frequency response study to investigate the vibratory response of a HMMWV vehicle over snow-covered obstacles. The study used a ground profile that changed as a function of time from 0 to 15 Hz over 60 seconds with an amplitude of 2.54 cm. A snow depth of 30.5 cm and density of 0.25 g/cc were used for the snow-covered conditions. The study found that the vehicle's body acceleration was attenuated at different rates based on the frequency of the road disturbance. At lower frequencies, below 8Hz, the snow cover attenuated the power spectral density of the body acceleration by approximately 2 dB. At higher frequencies of 14 Hz, the attenuation increased to 4 dB. The snow cover effectively lowered the vehicle's unsprung natural frequency by 1.5 Hz. The rut profile variation is reduced as frequency is increased, effectively reducing the ground profile variation that the vehicle traverses.

Vehicle mobility is an important consideration in any military operation enabling resupply to enemy engagement. The ability to better predict a vehicle's response to terrain allows for optimal path planning, resulting in safer and more efficient operations. Winter conditions, such as snow cover, can degrade vehicle mobility by reducing available traction and increasing motion resistance. Obstacles also reduce vehicle mobility by exceeding operator and equipment acceleration limits and adversely effecting lateral stability. In this study, we have shown that snow cover reduces the effect that obstacles have on vehicle mobility by reducing acceleration levels and normal force variation. We demonstrated the effects through experimental testing on a relatively high ground pressure wheeled vehicle (HMMWV) and through simulation models. A simulation study of a low ground pressure vehicle traversing snow-covered obstacles showed a large reduction in acceleration levels and normal force variation. Future mobility planning can use the predictive methods described in this study to make planning tools more accurate and ultimately result in more effective and safer military operations.

References

Blaisdell, G. L., P. W. Richmond, S. A. Shoop, C. E. Green, and R. G. Alger. 1990. *Wheels and Tracks in Snow: Validation Study of the CRREL Shallow Snow Mobility Model*. CRREL Report 90-9. Hanover, NH: U.S. Army Cold Regions Research and Engineering Laboratory. http://hdl.handle.net/11681/9109.

Karnopp, D. 1990. "Design Principles for Vibration Control Systems Using Semi-Active Dampers." *Journal of Dynamic Systems, Measurement, and Control* 112 (3): 448–455.

Mehmood, A., A. Khan, and A. Khan. 2014. "Vibration Analysis of Damping Suspension Using Car Models." *International Journal of Innovation and Scientific Research* 9 (2): 202–211.

Oppenheim, A. V., and R. W. Shafer. 1989. *Discrete-Time Signal Processing*. Upper Saddle River, NJ: Prentice Hall.

Pavlov, N. 2017. "Vibration Characteristics of Quarter Car Semi-Active Suspension Model—Numerical Simulations and Indoor Testing." *International Scientific Journal, Trans Motauto World* 2 (1): 11–16.

Richmond, P. W., S. A. Shoop, and G. L. Blaisdell. 1995. *Cold Regions Mobility Models*. CRREL Report 95-1. Hanover, NH: U.S. Army Cold Regions Research and Engineering Laboratory.

Richmond, P. W., G. L. Blaisdell, and C. E. Green. 1990. *Wheel and Tracks in Snow: Second Validation Study of the CRREL Shallow Snow Mobility Model*. CRREL Report 90-13. Hanover, NH: U.S. Army Cold Regions Research and Engineering Laboratory.

Shoop, S. A., M. Bodie, S. Frankenstein, M. Parker, and M. Bigl. 2019. "Recent Improvements to Snow Mobility Algorithms." In *Proceedings of the ISTVS 15th European-African Regional Conference*, Prague, Czech Republic, 9–11 September 2019.

Vecherin, S. N., J. M. Shaker, and M. W. Parker. 2020. *Obstacle Detection and Quantification for Vehicle Mobility in Winter Conditions*. ERDC/CRREL TR-20-7. Hanover, NH: U.S. Army Engineer Research and Development Center.

Welch, P. D. 1967. "The Use of Fast Fourier Transform for the Estimation of Power Spectra: A Method Based on Time Averaging over Short, Modified Periodograms.", IEEE Transactions on Audio and Electroacoustics 15 (2): 70–73.

REPORT DOCUMENTATION PAGE

Form Approved
OMB No. 0704-0188

1. REPORT DATE (DD-MM-YYYY)	2. REPORT TYPE	3. DATES COVERED (From - To)
November 2020	Technical Report / Final	FY18–FY21

4. TITLE AND SUBTITLE
Snow-Covered Obstacles' Effect on Vehicle Mobility

5a. CONTRACT NUMBER

5b. GRANT NUMBER

5c. PROGRAM ELEMENT
622145

6. AUTHOR(S)
Mark Bodie, Michael W. Parker, Alex Stott, and Bruce Elder

5d. PROJECT NUMBER
BG2

5e. TASK NUMBER
02

5f. WORK UNIT NUMBER

7. PERFORMING ORGANIZATION NAME(S) AND ADDRESS(ES)

U.S. Army Engineer Research and Development Center (ERDC)
Information Technology Laboratory (ITL)
72 Lyme Road
Hanover, NH 03755-1290

U.S. Army Engineer Research and Development Center (ERDC)
Cold Regions Research and Engineering Laboratory (CRREL)
72 Lyme Road
Hanover, NH 03755-1290

8. PERFORMING ORGANIZATION REPORT NUMBER
ERDC TR-20-26

9. SPONSORING / MONITORING AGENCY NAME(S) AND ADDRESS(ES)
Headquarters, U.S. Army Corps of Engineers
Washington, DC 20314-1000

10. SPONSOR/MONITOR'S ACRONYM(S)

11. SPONSOR/MONITOR'S REPORT NUMBER(S)

12. DISTRIBUTION / AVAILABILITY STATEMENT
Approved for public release; distribution is unlimited.

13. SUPPLEMENTARY NOTES
Mobility in Complex Environments

14. ABSTRACT

The Mobility in Complex Environments project used unmanned aerial systems (UAS) to identify obstacles and to provide path planning in forward operational locations. The UAS were equipped with remote-sensing devices, such as photogrammetry and lidar, to identify obstacles. The path-planning algorithms incorporated the detected obstacles to then identify the fastest and safest vehicle routes. Future algorithms should incorporate vehicle characteristics as each type of vehicle will perform differently over a given obstacle, resulting in distinctive optimal paths.

This study explored the effect of snow-covered obstacles on dynamic vehicle response. Vehicle tests used an instrumented HMMWV (high mobility multipurpose wheeled vehicle) driven over obstacles with and without snow cover. Tests showed a 45% reduction in normal force variation and a 43% reduction in body acceleration associated with a 14.5 cm snow cover. To predict vehicle body acceleration and normal force response, we developed two quarter-car models: rigid terrain and deformable snow terrain quarter-car models. The simple quarter models provided reasonable agreement with the vehicle test data. We also used the models to analyze the effects of vehicle parameters, such as ground pressure, to understand the effect of snow cover on vehicle response.

15. SUBJECT TERMS
Cold regions; Obstacles (Military science); Snow; Trafficability; Vehicles, Military

16. SECURITY CLASSIFICATION OF:			17. LIMITATION OF ABSTRACT	18. NUMBER OF PAGES	19a. NAME OF RESPONSIBLE PERSON
a. REPORT	b. ABSTRACT	c. THIS PAGE			19b. TELEPHONE NUMBER (include area code)
Unclassified	Unclassified	Unclassified	SAR	38	